Kinetics of decomposition in ionic solids: IV. Transition between nucleation and spinodal decomposition observed by time-resolved phonon spectroscopy

2005 J. Phys.: Condens. Matter 17 6559

(http://iopscience.iop.org/0953-8984/17/41/025)

INSTITUTE OF PHYSICS PUBLISHING JOURNAL OF PHYSICS: CONDENSED MATTER

J. Phys.: Condens. Matter **17** (2005) 6559–6573 doi:10.1088/0953-8984/17/41/025

Kinetics of decomposition in ionic solids: IV. Transition between nucleation and spinodal decomposition observed by time-resolved phonon spectroscopy

P Elter[1], G Eckold[1], H Gibhardt[1], W Schmidt[2,3] and A Hoser[3,4]

[1] Institut für Physikalische Chemie, Universität Göttingen, Germany
[2] Institut Laue-Langevin, Grenoble, France
[3] Institut für Festkörperforschung, Forschungszentrum Jülich, Germany
[4] Institut für Kristallographie, RWTH Aachen, Germany

Received 30 June 2005, in final form 5 September 2005
Published 30 September 2005
Online at stacks.iop.org/JPhysCM/17/6559

Abstract

Real-time inelastic neutron scattering has been used to study the kinetics of the demixing process in AgBr–NaBr mixed single crystals. The variation of transverse acoustic phonon spectra provides most direct information about the microscopic non-equilibrium behaviour. The phase separation is monitored by a well defined splitting of phonon peaks that reflects the different dynamical behaviours of the constituents. As a function of temperature, time evolution of the phonon spectra changes drastically, thus proving unambiguously that the demixing process is dominated by nucleation in the high-temperature regime and by concentration fluctuations at low temperatures.

1. Introduction

Silver alkali halides provide interesting model systems for the study of decomposition processes in ionic solids. This is not only due to simple phase diagrams and the absence of structural phase transitions but also to the invariance of the anion sublattice, which is not involved in the demixing process. The phase separation is entirely confined to the cationic system and the anions exhibit an almost rigid frame. Along with the strong polarizability of silver ions, this feature guarantees that even single crystals are not destroyed during demixing [1]. Hence, the process of phase separation can be studied on a microscopic scale using lattice vibrations—phonons—as a local probe. Since the elastic constants of NaBr and AgBr differ considerably, acoustic phonons are particularly suited for these investigations. As shown previously, time-resolved inelastic neutron scattering experiments are, in fact, feasible even on a timescale of seconds using stroboscopic techniques [2, 3]. This method provides most direct information about the variation of interatomic interactions associated with the decomposition process.

In a series of papers [3–7], it could be shown that at low temperatures, within the spinodal regime (for a review of the basic phenomena see e.g. [8–10]), two timescales can clearly be distinguished during the phase separation in the systems AgCl–NaCl and AgBr–NaBr: the chemical demixing due to the separation of the different types of cations takes place within minutes without changing the rigid lattice provided by the anions. This could be demonstrated by small angle scattering from concentration fluctuations [4, 5]. Moreover, the changes of local interactions in AgCl–NaCl mixed single crystals were directly determined in a first time-dependent phonon study [7]. Since the lattice parameters are conserved during this process considerable lattice strains are associated with the phase separation. Only on a much longer and temperature dependent timescale between hours and years are these lattice strains removed and the final equilibrium structures with different lattice parameters are obtained as observed by the splitting of Bragg reflections.

Due to the larger difference in lattice parameters of more than 3% in the bromide system [11], the strains are much more pronounced as compared to the chloride system. Hence, the coherent critical point is found at 458 K, which is almost 100 K below the incoherent one (558 K [12]), and the spinodal regime is strongly suppressed. In the metastable region of the phase diagram between spinodal and binodal, nucleation processes are believed to dominate the phase separation. Consequently, the correlation peak in small angle scattering, that is a characteristic feature of spinodal decomposition, disappears in this temperature regime [4].

In this paper, we will demonstrate that the time evolutions of transverse acoustic phonon spectra differ substantially in the two temperature regimes, thus proving the transition between the nucleation and fluctuation mechanism.

The paper is organized as follows. After describing some details of the experimental conditions, the concentration dependence of phonon frequencies in the homogeneous phase at 623 K is presented. The time evolution of phonon spectra after a quench into the fluctuation regime at 373 K and into the nucleation regime at 473 K are shown in the subsequent sections. The corresponding data are discussed in comparison with the findings obtained in the analogous chloride system. Finally, a short summary and outlook is given.

2. Experimental details

Large (cm^3) single crystals of $Ag_xNa_{1-x}Br$ with different compositions x were grown from the melt by the Czochralski method. Details are presented elsewhere [13]. For the present experiments, crystals with concentrations $x = 0.65$ (crystal A), 0.45 (crystal B) and 0.32 (crystal C) were used. Their quality was checked by gamma-ray diffraction, yielding mosaicities of 1.2°, 1.4° and 0.9°, respectively.

Specially designed furnaces were developed that were optimized for rapid cooling and heating in normal atmosphere. The crystals were wrapped in silver foil to guarantee temperature homogeneity.

The neutron scattering experiments were performed at the three-axis spectrometers UNIDAS (FRJ-2, Jülich) (static experiments) and IN12 (HFR, ILL-Grenoble) (kinetic experiments) using different combinations of neutron energy, collimation, etc. For the time-resolved investigations, a portable data acquisition system was developed that can be used with different spectrometers and is described in some detail in [13, 14]. During the experiments, the sample was periodically heated to the homogenization temperature of about 623 K and quenched to the decomposition temperatures. The initial quench rate was about 10–15 K s^{-1} and the final temperatures of 373 and 473 K were reached after about 10 and 50 s, respectively. The cycle period was chosen between 1000 and 10 000 s and the neutrons were counted in time channels of 10 s. In the fluctuation regime, the phonon spectra were averaged over three

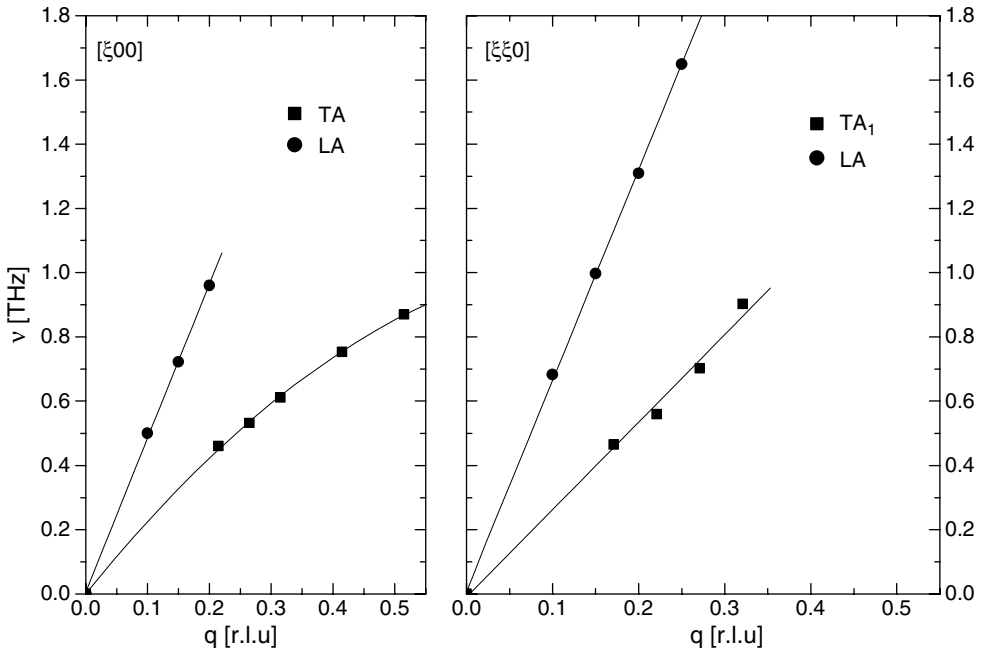

Figure 1. Low-frequency part of acoustic phonon dispersion in $Ag_{0.65}Na_{0.35}Br$ along [100] (left) and [110] (right) at 623 K. Note that the TA_1 phonon along [110] is polarized along [001].

time channels in order to improve the statistics, while in the nucleation regime averaging over 24 channels was possible without loss of information due to the different kinetic behaviour.

Most of the data were obtained observing the transverse acoustic phonon along [ξ00] at $\xi = 0.35$ or along [$\xi\xi$0] at $\xi = 0.2$. For comparison, the evolution of the (200) Bragg reflection was determined on the same timescale.

3. Results and discussion

3.1. Concentration dependence of transverse acoustic phonons in the homogeneous phase at 623 K

For crystal A ($x = 0.65$), the low-frequency part of the acoustic phonon dispersion along [ξ00] and [$\xi\xi$0] at 623 K is shown in figure 1. From the initial slopes of the different branches, the complete set of elastic constants is obtained:

c_{11}	40.8 GPa
c_{12}	27.7 GPa
c_{44}	8.1 GPa

Using crystals of different compositions, the concentration dependence of phonon frequencies could be determined. For the transverse acoustic phonon at [0.2 0 0] the results are summarized in figure 2. Note that the data of the pure compounds are taken from the literature [15, 16] and extrapolated to the temperature of 623 K with the help of the respective temperature coefficients of the elastic constant c_{44} ($T_{c_{44}}$(AgBr) $= -2.8 \times 10^{-4}$ K^{-1}, $T_{c_{44}}$(NaBr) $=$

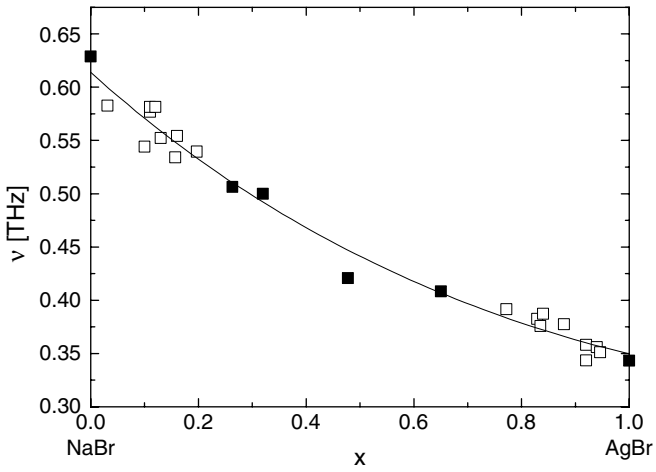

Figure 2. Concentration dependence of the TA[0.2 0 0] phonon frequency at 623 K. (The open symbols correspond to data obtained from demixed crystals and extrapolated to higher temperature by means of the temperature coefficients of elastic constants.)

-5.5×10^{-4} K^{-1} [17]). The phonon frequencies observed after complete demixing at lower temperatures (see below) are also included in figure 2 after extrapolation to 623 K.

Obviously, there is a non-linear variation of the mode frequencies with concentration. Even if this behaviour is less pronounced than in the chloride system [18], it can easily be seen that even small amounts of silver bromide introduced into the NaBr host lattice lead to a considerable softening of the lattice. The hardening of pure AgBr due to NaBr addition, on the other hand, is somewhat weaker. The non-linearity can be described in terms of elementary lattice dynamics, as demonstrated by Caspary *et al* [18].

In pure NaBr, the slope of the TA[100] acoustic phonon close to the Γ-point may be represented by

$$\left(\frac{\nu}{\xi}\right)^2 = \frac{1}{m_{\mathrm{Na}} + m_{\mathrm{Br}}} \sum_l [V_{\mathrm{NaNa},\,l} + 2V_{\mathrm{NaBr},\,l} + V_{\mathrm{BrBr},\,l}] \cdot z_l^2 = \frac{1}{m_{\mathrm{Na}} + m_{\mathrm{Br}}} V_{\mathrm{NaBr}}. \tag{1}$$

In this equation, ν is the frequency of the acoustic phonon with a wavevector ξ in reciprocal lattice units $(2\pi/a)$. $V_{ik,l}$ is the projection of the force constant matrix along the polarization direction for the interaction between ions i and k separated by a primitive lattice vector $\mathbf{r}_l$. z_l is the component of $\mathbf{r}_l$ along the phonon wavevector in units of the lattice parameter.

In mixed crystals with a statistical distribution of cations, this expression is replaced by

$$\left(\frac{\nu}{\xi}\right)^2 = \frac{1}{(x \cdot m_{\mathrm{Ag}} + (1-x) \cdot m_{\mathrm{Na}} + m_{\mathrm{Br}})} \cdot [-x^2 \cdot (\Delta V_{\mathrm{Ag}} + \Delta V_{\mathrm{Na}}) + 2x \cdot \Delta V_{\mathrm{Ag}} + V_{\mathrm{NaBr}}] \tag{2}$$

where the quantities ΔV_{Ag} and ΔV_{Na} are used to characterize the variation of the potential energy if a single sodium/silver ion is replaced by silver/sodium in the NaBr/AgBr matrix, respectively:

$$\Delta V_{\mathrm{Ag}} = \sum_l (V_{\mathrm{AgNa},\,l} - V_{\mathrm{NaNa},\,l} + V_{\mathrm{AgBr},\,l} - V_{\mathrm{NaBr},\,l}) \cdot z_l^2 \tag{3a}$$

$$\Delta V_{\mathrm{Na}} = \sum_l (V_{\mathrm{NaAg},\,l} - V_{\mathrm{AgAg},\,l} + V_{\mathrm{NaBr},\,l} - V_{\mathrm{AgBr},\,l}) \cdot z_l^2 \tag{3b}$$

$$\Delta V_{\mathrm{Ag}} + \Delta V_{\mathrm{Na}} = \sum_l (2V_{\mathrm{AgNa},\,l} - V_{\mathrm{AgAg},\,l} - V_{\mathrm{NaNa},\,l}) \cdot z_l^2. \tag{3c}$$

A least squares fit of the data presented in figure 2 to equation (2) yields the following results:

$$\Delta V_{Ag} = (-0.54 \pm 0.12)\ \mathrm{N\ m^{-1}}$$
$$\Delta V_{Na} = (0.12 \pm 0.11)\ \mathrm{N\ m^{-1}}$$
$$V_{NaBr} = (1.61 \pm 0.04)\ \mathrm{N\ m^{-1}}.$$

Obviously, the softening of the acoustic phonon branch with silver doping is not simply due to the larger mass of silver ions; instead, the short-range interactions of silver ions are significantly weaker than those of the sodium ions. Comparing the above data with the findings for the chloride system [18] ($\Delta V_{Ag} = (-1.37 \pm 0.17)$ N m^{-1}, $\Delta V_{Na} = (-0.34 \pm 0.35)$ N m^{-1}, $V_{NaCl} = (1.74 \pm 0.06)$ N m^{-1}) it is easily recognized that the effect of silver doping is considerably stronger in NaCl than in NaBr.

Since long range Coulomb interactions hardly change by the exchange of sodium with silver, the differences of the force constants are essentially due to the modifications of short range repulsive interactions. These are, however, determined by the polarizabilities of the individual ions as shown by the lattice dynamical investigations of Reid *et al* [15], Schmunk *et al* [19] or Singh *et al* [20]. According to the compilation of Tessman *et al* [21], the ionic polarizability of bromine ions ($\alpha_{Br} = 4.16$ Å^3) is considerably larger than that of chlorine ions ($\alpha_{Cl} = 2.96$ Å^3). Thus, the replacement of sodium ions ($\alpha_{Na} = 0.41$ Å^3) by the strongly polarizable silver ions ($\alpha_{Ag} = 2.4$ Å^3) will change the overall polarizability of the NaCl lattice much more than that of the NaBr lattice. The collective deformation of electron shells thus leads to a more pronounced softening of the NaCl lattice as compared to NaBr on doping with silver ions.

3.2. Phonons in demixed crystals

After complete demixing, the phonon spectra of $Ag_xNa_{1-x}Br$ crystals exhibit two well defined peaks corresponding to the two product phases as shown in figure 3. At 473 K, the TA[0.35 0 0] phonon of the sodium-rich phase is observed at about 0.9 THz, while that of the silver-rich phase is located at 0.6 THz. The integrated intensities of both peaks correspond to the volume fractions of the demixed phases as obtained from the lever rule and the respective inelastic structure factors. For comparison, the single phonon of the homogeneous phase that is centred at about 0.75 THz (crystal C, $x = 0.32$) is also shown in this figure. The lower part of figure 3 displays spectra of the TA[0.2 0.2 0] phonon obtained for crystal B with larger overall silver concentration ($x = 0.45$) at 373 K.

If a demixed crystal is heated continuously, remixing leads to a shift of the two phonons on the frequency scale. Taking into account the temperature dependence of the sound velocities of the constituents, the concentrations of the coexisting phases can be determined from the phonon spectra using the master curve of figure 2. These results are in very good agreement with the concentrations obtained from the splitting of Bragg reflections after long-time ageing. Comparing these data, however, with the equilibrium phase diagram known from the literature [11, 12, 22], it is found that the miscibility gap is somewhat reduced. It will be shown below that this finding is due to residual coherency stresses, which are not removed by thermal ageing but only by mechanical treatment.

3.3. Evolution of phonon spectra after quenching to 373 K

The time evolution of phonon spectra from the initial to the final state gives direct information about the underlying mechanism. Figure 4 shows the variation of transverse acoustic phonon spectra for crystal B ($x = 0.45$) at $\mathbf{q} = (0.2\ 0.2\ 0)$ after quenching from 623 to 373 K,

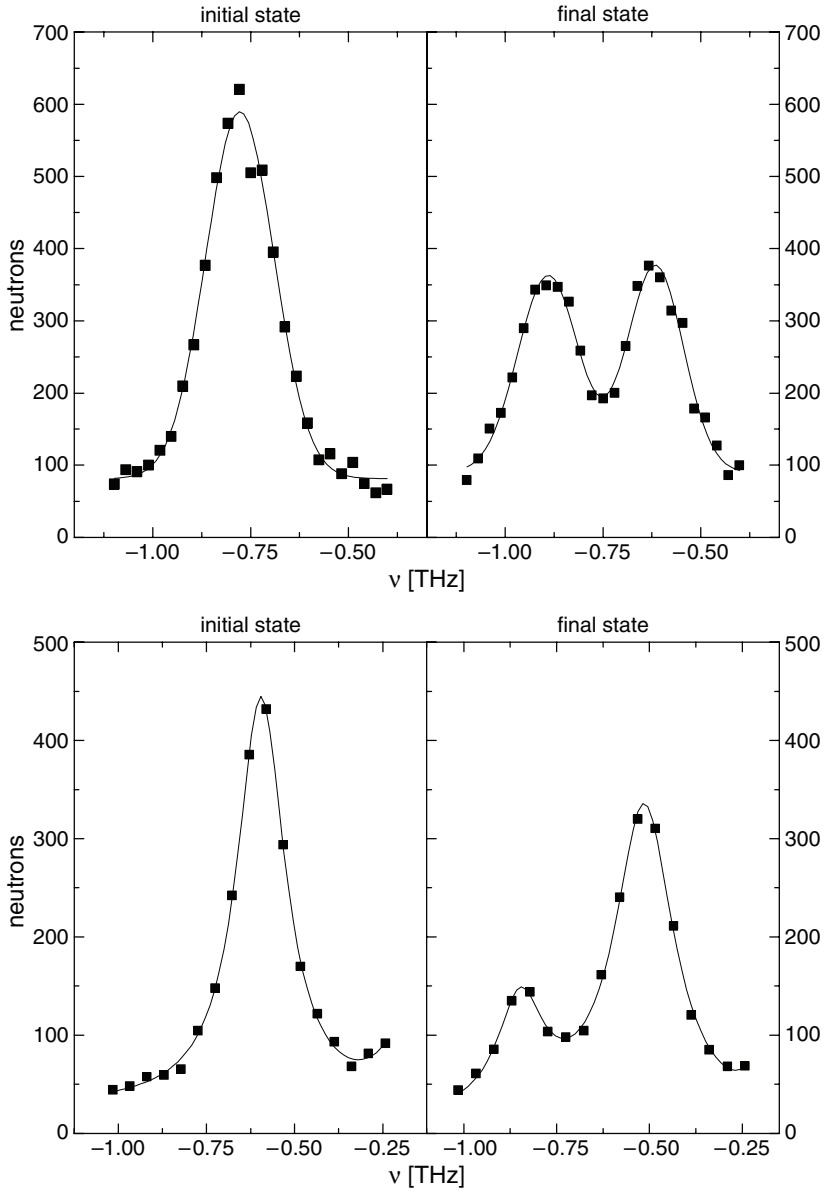

Figure 3. Transverse acoustic phonons in demixed crystals: top, TA[0.35 0 0] in $Ag_{0.32}Na_{0.68}Br$ (crystal C) at 473 K; bottom, TA_1 [0.2 0.2 0] (polarized along [001]) in $Ag_{0.45}Na_{0.55}Br$ (crystal B) at 373 K.

which is about 180 K below T_c. The start of the quench defines the time zero. In order to improve the counting statistics the phonon spectra are summed up over three time channels, thus representing a time average over 30 s. The final temperature was reached after about 50 s. The spectrum at $t = 45$ s therefore corresponds to the cooling period and shows essentially the phonon of the homogeneous phase with composition $Ag_{0.45}Na_{0.55}Br$ centred at 0.60 THz. In the next time-step, at 75 s, a clear splitting into two components is already observed. The

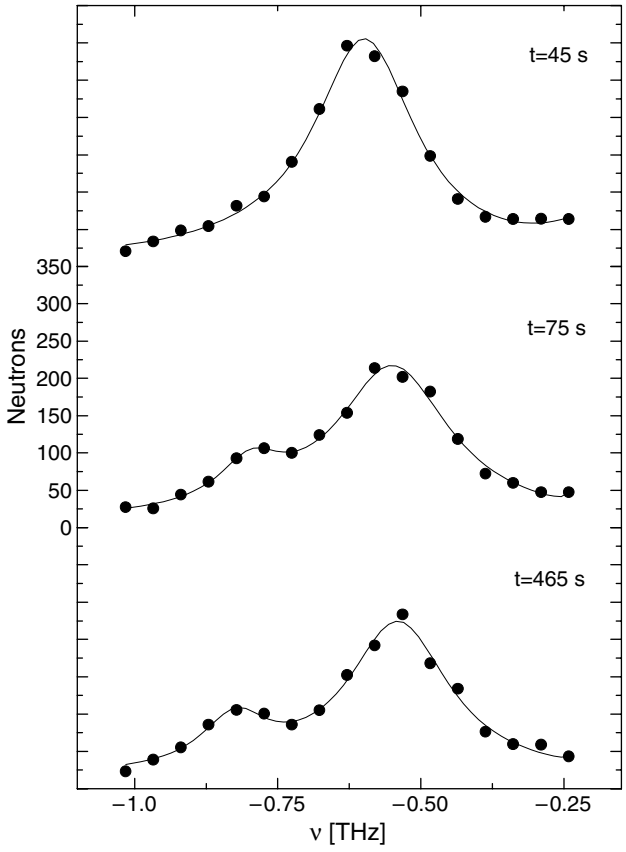

Figure 4. Time evolution of the $TA_1[0.2\ 0.2\ 0]$ phonon in $Ag_{0.45}Na_{0.55}Br$ during demixing at 373 K. (The lines are the results of a fit with two Lorentzians, except for the spectrum at $t = 45$ s, which corresponds to the homogeneous state.)

separation of these two phonon peaks proceeds subsequently and, hence, two well defined phonons at 0.55 THz (silver-rich phase) and 0.8 THz (sodium-rich phase) are detected after 465 s. Obviously, demixing takes place on this rather short timescale of seconds or a few minutes. At longer times, there is only a minor shift of the individual peaks as demonstrated in figure 5.

It should be noted that the increase of the intensity of the low-frequency peak is entirely due to the variation of the inelastic structure factor (that is inversely proportional to the square of the frequency), rather than to an increase of the phase volume. The phonon spectra can well be fitted to the sum of two Lorentzians as demonstrated in figures 4 and 5. The evolution of the peak frequencies is presented in figure 6. It is readily seen that the phonon splitting, in fact, takes place within a short time interval of about 200 s after quenching. There is, however, a second stage of the demixing process associated with a continuous shift of the phonon frequencies on a timescale of hours.

The phonon line widths are of particular interest since they may provide information about the damping of lattice vibrations in inhomogeneous systems. Due to the limited counting statistics, however, the present results do not allow us to determine the line widths very accurately. The most that can be said is that during ageing, there seems to be a trend towards

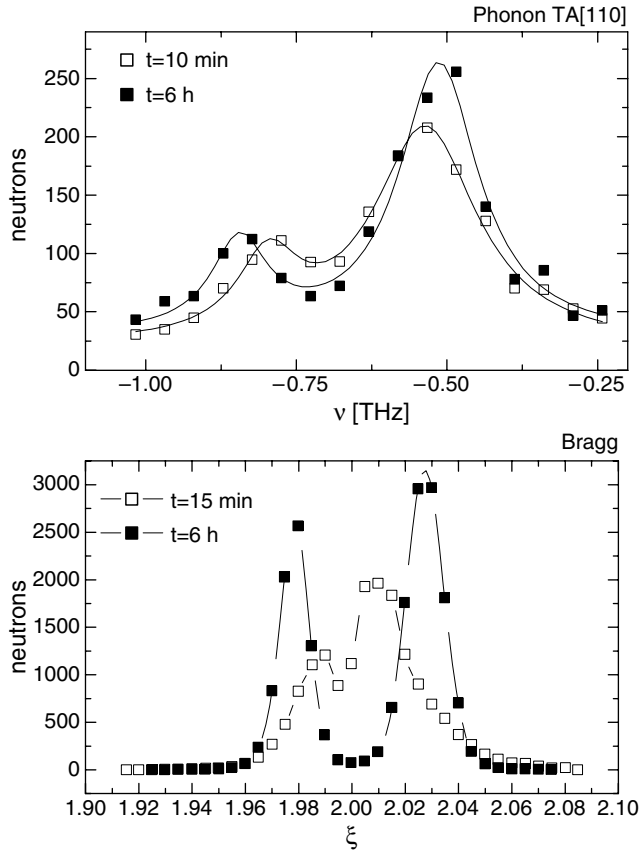

Figure 5. Long-time behaviour of the $TA_1[0.2\ 0.2\ 0]$ phonon (top) and the (002) Bragg peak (bottom) in $Ag_{0.45}Na_{0.55}Br$ during demixing at 373 K. (The phonon spectra are fitted to the sum of two Lorentzians, while the lines of the Bragg profile are guides to the eye only.)

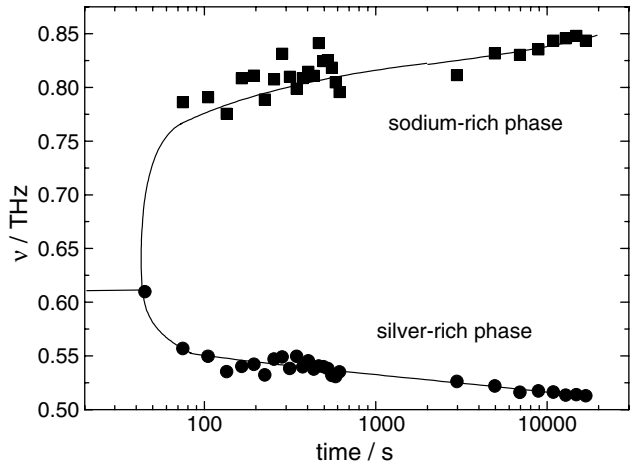

Figure 6. Time evolution of $TA_1[0.2\ 0.2\ 0]$ phonon frequencies at 373 K.

sharper phonon lines for the silver-rich component, in particular. In future experiments, the phonon damping during decomposition will be investigated in detail.

Similar to the findings in the AgCl–NaCl system [7], the Bragg reflections exhibit a different time evolution compared to the phonon spectra. As shown in the lower part of figure 5, a rather broad intensity distribution is observed after several minutes. Only after a period of more than two hours are two well defined and separated Bragg peaks of the product phases found. These results are in close agreement with previous powder experiments [4]. It confirms the fact that chemical demixing within the cation sublattice takes place at almost constant lattice parameter that is essentially determined by the anions. The relaxation of the lattice, i.e. the contraction of silver-rich domains and the expansion of sodium-rich ones, occurs only in a subsequent step and needs a much longer time to proceed.

The different time evolutions of phonons and Bragg reflections can be illustrated with the help of time auto-correlation functions, as defined by

$$C(t) = \frac{\int I(x,t) \cdot I(x,t_0)\,\mathrm{d}x}{\int (I(x,t_0))^2\,\mathrm{d}x} \tag{4}$$

where x is the scan variable, i.e. the frequency in phonon scans and the wavevector in longitudinal scans across Bragg peaks. t_0 is taken as the time when the decomposition temperature is reached in order to separate effects of cooling. The correlation function thus describes the change of intensity profiles with time and provides a quantitative measure for the time evolution. The time dependence of this correlation function is presented in the upper part of figure 7 for acoustic phonons as well as Bragg reflections. It is readily seen that the timescales differ by more than one order of magnitude. While the phonons show well defined splitting after some 100 s, the Bragg peaks need more than 2000 s to separate. This finding may be compared to the results from small angle scattering that yield a correlation peak which is characteristic for spinodal decomposition. The time dependence of integrated small angle intensity and of the position of the correlation peak as obtained from [4] is therefore included in figure 7. Obviously, the development of the correlation peak and that of the phonon spectra go hand in hand, while the lattice relaxation that is characterized by Bragg reflections is delayed.

Compared to the analogous chloride system, it is found that the timescale for phase separation is almost the same while that for the lattice relaxation is considerably shorter. It was shown by Caspary [18] that in AgCl–NaCl crystals even after several years the Bragg profiles still consist of a broad intensity distribution rather than of two well defined peaks of the product phases. The different behaviour of the bromide system can be attributed to the larger lattice parameter mismatch, which is 3.4% in AgBr–NaBr but only 1.7% in AgCl–NaCl. Hence, the driving force for lattice relaxation is significantly larger in AgBr–NaBr. This is also the reason why satellites close to the Bragg reflections due to concentration fluctuations could not be detected in the present system.

It should be noted, however, that even after more than 2 days, when the Bragg profiles become time independent and consist of two well separated components (see the bottom part of figure 5), the lattice has not yet reached a true equilibrium state. There is evidence that the crystals still exhibit appreciable residual internal strains. X-ray powder experiments show that the Bragg peaks of the product phases are much broader than the experimental resolution, as displayed in figure 8. Only after additional mechanical grinding of the decomposed samples in a mortar could sharp peaks be observed that show the Cu Kα1/Kα2 fine structure. This finding indicates that residual strains can be removed only by mechanical treatment and not simply by thermal ageing.

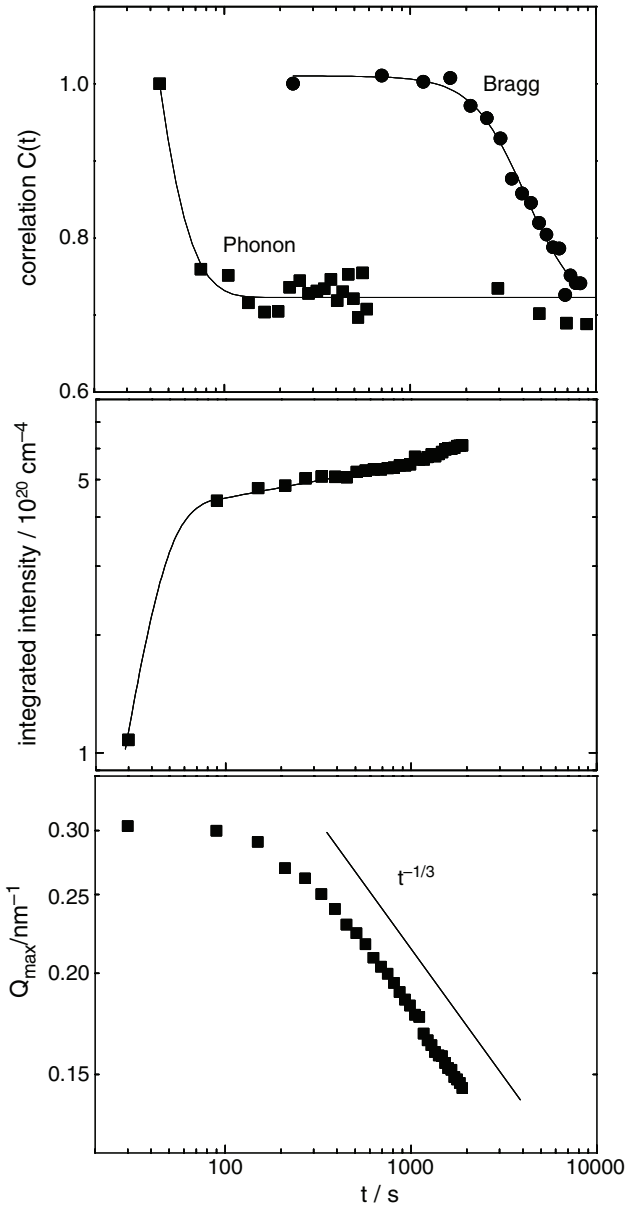

Figure 7. Time dependence of the autocorrelation function for phonons and Bragg reflections (top), integrated small angle intensity (middle) and position of correlation peak (after [4]) during demixing at 373 K.

3.4. Evolution of phonon spectra after quenching to 473 K

Since the coherent critical point of the AgBr–NaBr system (458 K) is found almost 100 K below the incoherent one [4], this system offers the possibility to investigate the changes in decomposition mechanism when leaving the fluctuation (spinodal) regime and entering the nucleation regime. Figure 9 displays the time evolution of the TA[0.35 0 0] phonon in a single

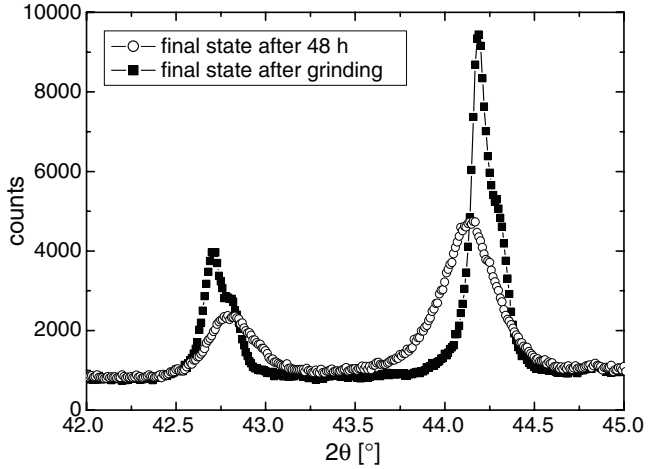

Figure 8. X-ray powder diffraction after long ageing time before and after mechanical grinding.

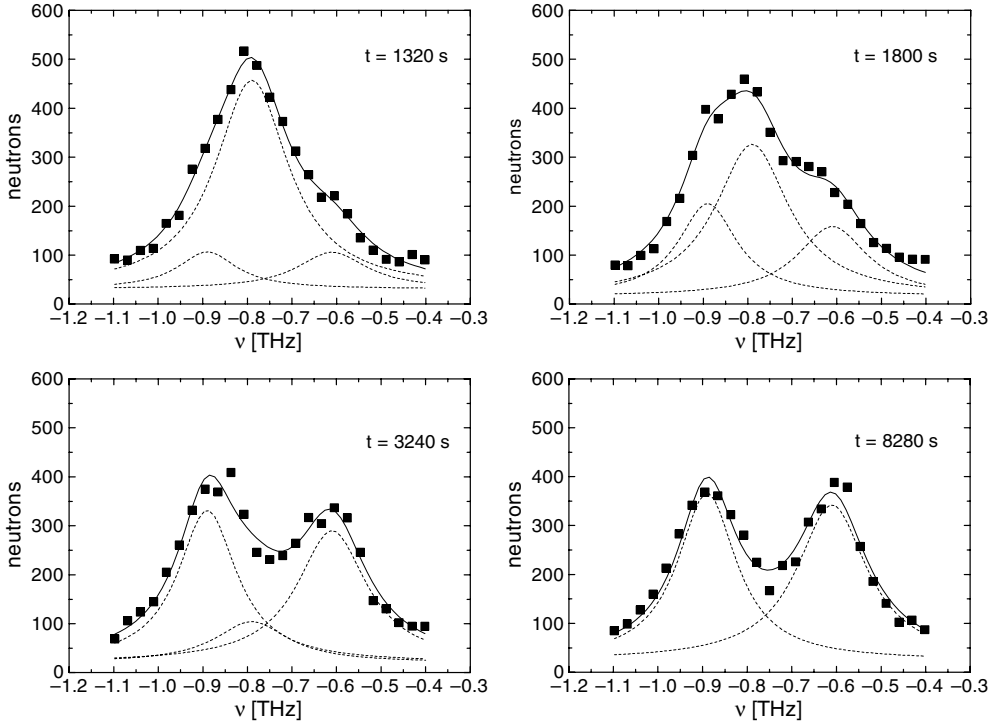

Figure 9. Time evolution of the TA[0.35 0 0] phonon in $Ag_{0.32}Na_{0.68}Br$ during demixing at 473 K. (The lines are the results of a fit with three (two) Lorentzians.)

crystal of composition $Ag_{0.32}Na_{0.68}Br$ at 473 K. It is readily recognized that the timescale of phonon variation is much longer as compared to the behaviour in the fluctuation regime. At 473 K, the splitting of the phonon into two well defined peaks is completed only after several thousand seconds. In the intermediate time, the intensity profiles can be fitted to

the sum of three components corresponding to the parent phase (at 0.79 THz) and the two product phases (at 0.61 THz and 0.89 THz, respectively) just as expected for the nucleation mechanism. In order to reduce the statistical errors, the phonon line widths have been fixed during the fitting procedure at 0.20 THz for the parent phase and 0.19 THz/0.16 THz for the two product phases. These values are slightly larger than the resolution of the spectrometer, which seems reasonable in view of the anharmonicity of the system. Being a superposition of three individual Lorentzians, the spectra are qualitatively different from those obtained in the fluctuation regime at 373 K and reflect the change in the mechanism of demixing from fluctuation towards nucleation. The integrated intensities can be used to calculate the volume fractions of the different phases. To this end, the variation of the dynamical structure factor with frequency and concentration has to be considered. In the temperature and frequency regime of the present experiment, the phonon intensity varies proportionally to the inverse square of the frequency. Moreover, it is proportional to the square of the mean scattering length of each particular phase. Hence, the experimentally determined integrated intensities for phonons of the different phases j ($j = 0$, parent phase; $j = 1$, sodium-rich phase; $j = 2$, silver-rich phase) are corrected via the following equation:

$$I_{j,\mathrm{corr}} = \left(\frac{\nu_i}{x_j b_{\mathrm{Ag}} + (1 - x_j) b_{\mathrm{Na}} + b_{\mathrm{Br}}} \right)^2 I_j \tag{5}$$

(with the coherent scattering lengths $b_{\mathrm{Ag}} = 0.59 \times 10^{-12}$ cm, $b_{\mathrm{Na}} = 0.36 \times 10^{-12}$ cm, $b_{\mathrm{Br}} = 0.68 \times 10^{-12}$ cm). The compositions of the product phases are taken from the incoherent miscibility gap as $x_1 = 0.15$ and $x_2 = 0.81$, while $x_0 = 0.32$ is the overall composition of the sample. Neglecting possible differences in the Debye–Waller factors, $I_{j,\mathrm{corr}}$ is proportional to the volume of phase j. The time evolutions of the corrected intensities are displayed in figure 10. Note that the sum $I_{0,\mathrm{corr}} + I_{1,\mathrm{corr}} + I_{2,\mathrm{corr}}$ is independent of time, which can be regarded as a justification of the present analysis. The degree of decomposition α may be calculated as

$$\alpha = \frac{I_{1,\mathrm{corr}} + I_{2,\mathrm{corr}}}{I_{0,\mathrm{corr}} + I_{1,\mathrm{corr}} + I_{2,\mathrm{corr}}} \tag{6}$$

and is shown in the lower part of figure 10. The data can be fitted to a stretched exponential behaviour according to an Avrami law

$$\alpha(t) = 1 - \exp(-(t/t_0)^{\beta}) \tag{7}$$

with $t_0 = (2200 \pm 20)$ s and $\beta = (2.56 \pm 0.08)$. An exponent 5/2 is characteristic for diffusion controlled growth rate of spherical nuclei, e.g. [8]. Moreover, t_0 characterizes the timescale of demixing, which is thus one order of magnitude larger than in the fluctuation regime below 458 K.

In agreement with this interpretation we also found that the Bragg profiles consist of three individual components as shown in figure 11 and differ thus qualitatively from the spectra obtained in the spinodal regime (see figure 5). Well defined peaks corresponding to the different phases can be distinguished from the very beginning of the phase separation. A quantitative phase analysis on the basis of the Bragg data could, however, not be achieved since it needed a complete 3D peak profile analysis in order to provide reliable integrated intensities which was not possible within the available beam time. The timescale on which the Bragg profiles evolve is, however, in very good agreement with the change of the phonon spectra. Hence, phonons and Bragg reflections go hand in hand, which is further proof for a simple nucleation mechanism.

It should be noted that time-resolved powder data have been obtained previously on samples with larger concentration of silver bromide ($Ag_{0.45}Na_{0.55}Br/Ag_{0.5}Na_{0.5}Br$) [4]. Under fast quenching conditions, small angle scattering as well as powder diffraction yielded a kinetic

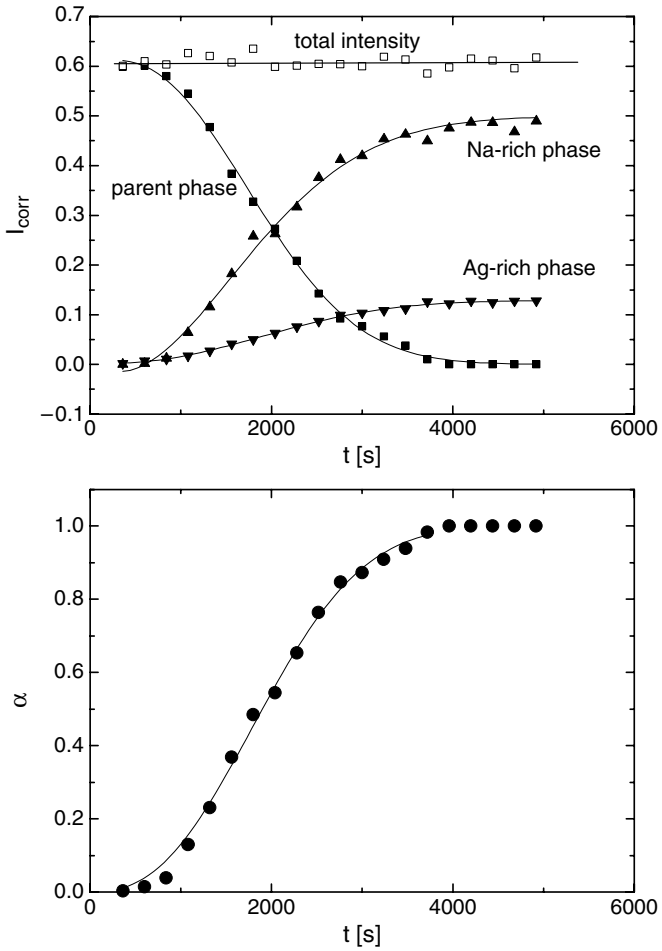

Figure 10. Time dependence of the phonon intensities (top) and the degree of decomposition (bottom) during demixing of $Ag_{0.32}Na_{0.68}Br$ at 473 K. The lines are fits to an Avrami equation.

behaviour in the nucleation regime that is equally well described by an Avrami equation with exponent $\beta \approx 5/2$. The time constant was, however, considerably shorter (about 500 s) than that observed in the present single-crystal experiments. The enhanced kinetics in powder specimens might be due to grain boundary diffusion or preferred nucleation at grain boundaries.

4. Conclusion

On a timescale of seconds, the time evolution of phonon spectra was observed in mixed single crystals of AgBr and NaBr after quenching into the miscibility gap using stroboscopic real-time inelastic neutron scattering. It could be shown that the lattice vibrations, as fingerprints of the local interatomic forces, provide direct information about the underlying mechanism of phase separation.

As a reference for real-time investigations, the concentration dependence of transverse acoustic phonon spectra in the homogeneous high-temperature phase has been determined. It could be shown that there is a significant softening of the NaBr lattice by AgBr doping. This

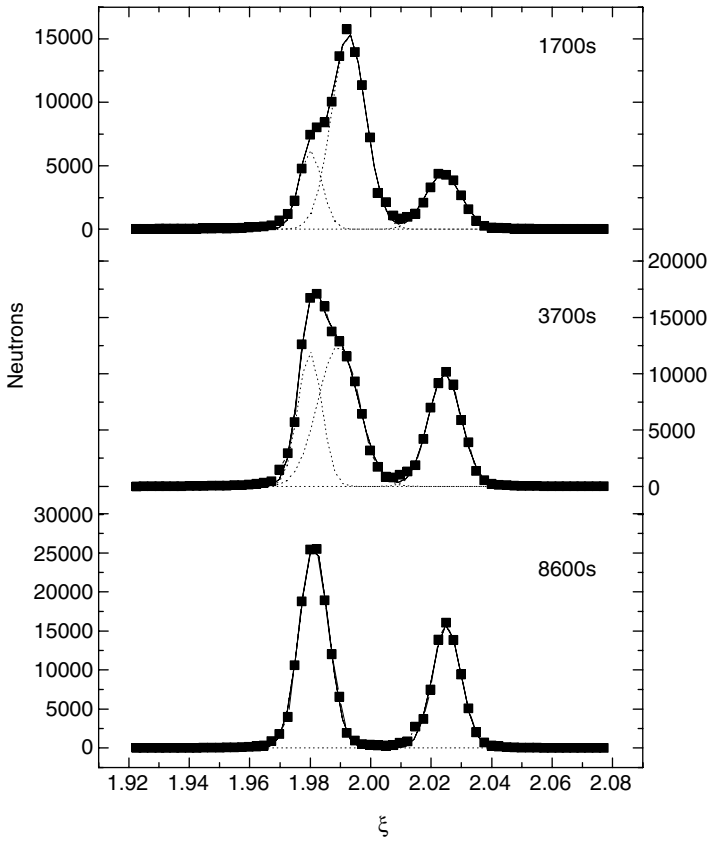

Figure 11. Time evolution of the (200) Bragg reflection of $Ag_{0.32}Na_{0.68}Br$ at 473 K.

effect is, however, considerably weaker compared to the analogous chloride system due to the different electronic polarizabilities.

After quenching deep into the miscibility gap, the phonon spectra change immediately on a timescale of seconds or minutes as soon as the temperature regime of spinodal decomposition below 458 K is entered. Similar to the chloride system that has been investigated previously, concentration fluctuations govern the phase separation. The lattice relaxation, however, that is associated with the splitting of Bragg reflections due to the different lattice parameters of the product phases is a subsequent step of the demixing process and occurs on a timescale of hours. But even after long ageing times internal mechanical strains persist, which can only be released by mechanical treatment like grinding.

In the metastable regime of the phase diagram between the spinodal and the incoherent miscibility gap (binodal), the time evolutions of phonons and Bragg reflections go hand in hand. Phonon spectra as well as Bragg profiles can be described by three well defined components corresponding to the parent and the two product phases as expected from a simple nucleation mechanism. The phonon intensities can be used to calculate the volume fractions and the degree of decomposition as a function of time. The kinetic behaviour follows an Avrami law with a characteristic exponent of about $5/2$ as expected for diffusion controlled processes.

The ionic system AgBr–NaBr thus provides an almost ideal model system for the study of different mechanisms of decomposition. Real-time inelastic scattering from phonons has

proven to be a powerful method to monitor the transition between fluctuation and nucleation controlled regimes. More generally, stroboscopic techniques in combination with neutron scattering provide interesting new possibilities for the investigation and characterization of transient non-equilibrium states in solids, be these induced by periodic temperature changes, mechanical loads or electric or magnetic fields.

References

[1] Windgasse J, Eckold G and Güthoff F 1997 *Physica* B **234–236** 153
[2] Gibhardt H, Eckold G and Güthoff F 2000 *Physica* B **276–278** 240
[3] Eckold G, Caspary D, Elter P, Güthoff F, Hoser A and Schmidt W 2004 *Physica* B **350** 83–6
[4] Eckold G 2001 *J. Phys.: Condens. Matter* **13** 217
[5] Caspary D, Eckold G, Güthoff F and Pyckhout-Hintzen W 2001 *J. Phys.: Condens. Matter* **13** 11521
[6] Elter P, Eckold G, Caspary D, Güthoff F and Hoser A 2002 *Appl. Phys.* A **74** S1179–71
[7] Eckold G, Caspary D, Gibhardt H, Schmidt W and Hoser A 2004 *J. Phys.: Condens. Matter* **16** 5945–54
[8] Raghavan V and Cohen M 1975 *Treatise on Solid State Chemistry* vol 5, ed A Hannay (New York: Plenum) p 67
[9] Gunton J D, San Miguel M and Sahni P S 1983 *Phase Transitions and Critical Phenomena* vol 8, ed C Domb and J L Lebowitz (London: Academic) p 267
[10] Komura S 1988 *Phase Transit.* **12** 3
[11] Trzeciok D and Nölting J 1980 *Z. Phys. Chem.* **119** 183
[12] Sinistri C, Riccardi R, Margheritis C and Tittarelli P 1971 *Z. Naturf.* a **27** 149
[13] Elter P 2003 *Thesis* Göttingen University
[14] Eckold G, Gibhardt H, Caspary D, Elter P and Elisbihani K 2003 *Z. Kristallogr.* **218** 154
[15] Reid J S, Smith T and Buyers W J L 1970 *Phys. Rev.* B **1** 1833
[16] Bührer W 1975 *Phys. Status Solidi* b **68** 739
[17] Every A G and McCurdy A K 1992 *Landolt-Börnstein New Series* vol 29, ed D F Nelson (Berlin: Springer) p 240
[18] Caspary D, Eckold G, Elter P, Gibhardt H, Güthoff F, Demmel F, Hoser A, Schmidt W and Schweika W 2003 *J. Phys.: Condens. Matter* **15** 6415
[19] Schmunk R E and Winder D R 1970 *J. Phys. Chem. Solids* **31** 131
[20] Singh R K and Chandra K 1976 *Phys. Rev.* B **14** 2625
[21] Tessman J R, Kahn A H and Shockley W 1953 *Phys. Rev.* **92** 890
[22] Tsuji T, Fueki K and Mukaibo T 1969 *Bull. Chem. Soc. Japan* **42** 2193